DYNAMIC MODELING OF FILAMENTOUS BULKING IN LAB-SCALE ACTIVATED SLUDGE PROCESSES

E.N. Banadda, I.Y. Smets, R. Jenné, and J.F. Van Impe*

Chemical Engineering Department
Katholieke Universiteit Leuven, B-3001 Leuven (Belgium)
Fax: +32-16-32.29.91
e-mail: jan.vanimpe@cit.kuleuven.ac.be

*Corresponding author

Abstract: Activated sludge is a complex ecosystem constituted mainly of bacteria and protozoa. Filamentous bulking, a phenomenon when the filamentous organisms dominate the activated sludge is still a widespread problem in the operation of activated sludge processes. Image analysis offers promising perspectives for early detection of filamentous bulking because the morphology parameters of the activated sludge react very fast to changing process conditions. This paper is aimed at identifying dynamic ARX and state space models as a function of organic loading and digital image analysis information (such as the total filament length per image and some representative mean floc shape parameters) to describe the evolution of the Sludge Volume Index (SVI). Their performances are compared based on an adequate quality performance criterion.

Keywords: Environmental engineering, image analysis, modeling, monitoring.

1. INTRODUCTION

Activated sludge systems encompass biodegradation and sedimentation processes which take place in the aeration and sedimentation tanks, respectively. The performance of the activated sludge process is, however, to a large extent dictated by the ability of the sedimentation tank to separate and concentrate the biomass from the treated effluent. Since the effluent from the secondary clarifier is most often not treated any further, a good separation in the settler is critical for the whole plant to meet the effluent standards. Apart from bad operating strategies or poorly designed clarifiers, settling failures can be mainly attributed to *filamentous bulking*. As a general guideline, filamentous bulking is said to occur when the Sludge Volume Index [1] (SVI) is greater than 150mLg^{-1}, regardless of its cause. Apart from the physico-chemical parameters, biological parameters are also increasingly consulted through microscopic observation. However, microscopic observation is not only subjective (i.e., operator dependent) but also time consuming, often leaving insufficient time for corrective interventions. Image analysis, a computer assisted procedure through which analysis of digital images is performed, could provide an objective means to assist the operator's decision making. Furthermore, mathematical models, capable of predicting the evolution of, e.g., the SVI value, will be indispensable for the development of early warning and detection tools. Although filamentous bulking has been studied intensively during the last decades (Jenkins *et al.*, 1993), the phenomenon is so complex (i.e., influenced by so many different factors) that a first principles model is still lacking. The identification of a model to predict in real-time - with reasonable accuracy - the appearance of sludge bulking is therefore of great importance, in view of the potential for improvement in plant efficiency and cost saving (Novotny *et al.*, 1990). This paper aspires to identify ARX and state space type models which can predict the settling characteristic SVI as a function of either organic loading (Q) and/or digital image analysis information as will be explained later on. The model performances are compared based on a quality performance criterion. Since static (instantaneous) correlation models, as reported by, e.g., da Motta and coworkers (da Motta *et al.*, 2002) cannot provide future SVI predictions nor take into account the system's delay, we will focus on *dynamic* models. In other words, we focus on how the past input data, i.e., in this case organic loading and/or digital image analysis information, affect(s) the future

[1] volume in milliliters occupied by 1 g of a suspension after 30 minutes settling

output data, i.e., the SVI. In a first approach *linear* models (ARX and state space models) have been preferred over *nonlinear* ones in modeling the filamentous bulking phenomena although the latter could be characterized by nonlinear behavior (since living organisms are involved). Linear model identification is however a much more *mature* field.

2. MATERIALS AND METHODS

This study relies on results obtained from two laboratory wastewater treatment experiments. Both systems are operated under more or less similar conditions so as to mimic a large-scale continuous system. However, it is worth mentioning that for both experiments, conditions were chosen to favor filamentous bulking outbreaks (Jenné *et al.*, 2003; Banadda *et al.*, 2003).

2.1 Lab-scale activated sludge system

The laboratory set-up is a continuous type activated sludge system in a classic configuration: an aeration tank (5.5 L) followed by a sedimentation tank (3 L) and sludge recycle (Figure 1).

Fig. 1. Left: lab-scale activated sludge system. Right: microscope (Olympus BX51) and video camera (Sony DXC-950P) used for daily capturing of activated sludge images.

This system was inoculated with activated sludge from a domestic wastewater treatment plant at Huldenberg (Belgium). The influent was synthetic wastewater, nevertheless, different feed regimes and carbon sources were administered (Figure 2), i.e., the use of glucose in the second experiment as opposed to sodium acetate (first experiment) aimed at inducing earlier filamentous bulking outbreaks. Quantitative information which includes analytical results of the effluent quality are recorded: organic matter, measured as Chemical Oxygen Demand (COD), the settleability measured as Sludge Volume Index (SVI), the activated sludge concentration measured as the Mixed Liquor Suspended Solids (MLSS) and the effluent Suspended Solids (SS). Also, digital image analysis is performed on a daily basis on 50 images per sample as reported in previous studies (Jenné *et al.*, 2002). The first experiment lasted 70 days while the second lasted 38 days (see Figure 2).

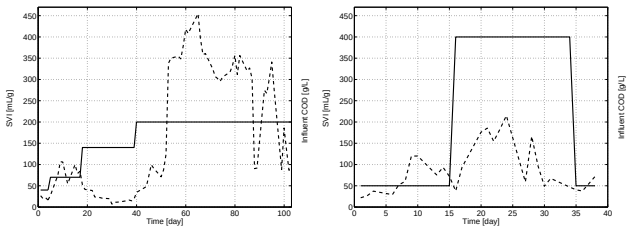

(a) (b)

Fig. 2. Evolution of the SVI (- - -) and influent COD feed regime (—) for (a) the first experiment and (b) the second experiment.

2.2 Image analysis procedure

Images of activated sludge samples were recorded by means of a light microscope (Olympus BX51) with phase contrast equipped with a 3CCD color video camera (Sony DXC-950P), shown in Figure 1. The magnification of the microscope objective used was 10×10 times. A fully automatic image analysis method for recognition and characterization of flocs and filaments in an activated sludge sample has been developed in previous work (Jenné *et al.*, 2002; Jenné *et al.*, 2003), and is applied to all colored phase contrast images.

2.3 Measurements

The principal aim of the image processing procedure is the extraction of certain information from the digital images. Once the objects in the image (i.e., the flocs and the filaments) are distinguished from the background, several size and shape related parameters can be computed.

Filament measurement. The filament length per image (F) describes the total length of the filament skeleton.

Floc size measurement. The size of the sludge flocs is an important parameter with respect to the settling properties (Ganczarczyk, 1994). The size of the flocs is expressed as the equivalent circle diameter D_{eq}, calculated from the real projected area A:

$$D_{eq} = 2\sqrt{A/\pi} \tag{1}$$

Floc shape measurements. It is mentioned in the literature (Eriksson and Hardin, 1984) that the shape of sludge flocs is related to the settling properties. Many shape quantifying parameters can be measured by means of image analysis. Four parameters are considered in this study.

- The form factor (FF) is particularly sensitive to the *roughness* of the boundaries. A circle has an FF value equal to one.

$$\mathrm{FF} = 4\pi \frac{\text{area}}{\text{perimeter}^2} \tag{2}$$

- The aspect ratio (AR) is mainly influenced by the elongation of an object. It varies between 1 and infinity. A circle has an AR value equal to one.

$$\text{AR} = 1 + \frac{4 \cdot (\text{Length-width})}{\pi.\text{width}} \quad (3)$$

- The roundness (R) is also mainly influenced by the elongation of an object. It varies between 0 and 1. A circle has an R value equal to one.

$$\text{R} = \frac{4 \cdot \text{area}}{\pi.\text{length}^2} \quad (4)$$

- The reduced radius of gyration (RG) is also influenced by the elongation of an object. A more elongated floc will have a larger RG. A circle has an RG value equal to $\frac{\sqrt{2}}{2}$.

$$\text{RG} = \frac{\sqrt{M_{2x} + M_{2y}}}{\frac{D_{eq}}{2}} \quad (5)$$

M_{2x} and M_{2y} are second order moments.

3. EXPERIMENTAL RESULTS AND DISCUSSION

Previous studies by Jenné *et al* (2003), have shown that a reasonably good correlation exists between the digital image analysis information and the SVI. In this paper, new model inputs in addition to those mentioned in (Banadda *et al.*, 2003), are investigated. Data collected during the two experimental periods are used to identify ARX and state space models that describe the SVI evolution, i.e., the model output, based on either (*i*) information gathered with the image analysis procedure (i.e., F, FF, D_{eq}, R, RG) and/or (*ii*) the organic loading (Q) profile as the model inputs. Afterwards the identified models from one experiment are cross-validated on the data of the other experiment.

3.1 Optimization criterion

The criterion to be maximized is the *R-squared adjusted* (R^2_{adj}) value, which is often expressed in percent (Equation (6)). The values obtained from the criterion reflect the percentage of output variation explained by the model (i.e., $y_h(t)$). Moreover, the R^2_{adj} criterion takes into account both the number of data points N and the model parameters (degrees of freedom) DF.

$$R^2_{adj} = 100 \cdot \left(1 - \frac{(N-1) \cdot \sum_{t=1}^{N} (y(t) - y_h(t))^2}{(N - DF) \cdot \sum_{t=1}^{N} (y(t) - mean(y(t)))^2}\right) \quad (6)$$

with $y(t)$ the measured output at discrete time t, $y_h(t)$ the model output at discrete time t.

3.2 ARX models

Procedure. ARX models relate the current output $y(t)$ to a finite number of past outputs $y(t-k)$ and inputs $u(t-k)$.

$$y(t) + a_1 y(t-1) + (\cdots) + a_{na} y(t-na) = b_1 u(t-nk) + b_2 u(t-nk-1) + (\cdots) + b_{nb} u(t-nk-nb+1) + e(t) \quad (7)$$

with $y(t)$ equal to the output response at discrete time t, $u(t)$ the input at discrete time t, na the number of poles, nb the number of zeros, nk the pure time-delay (the dead-time) in the system and $e(t)$ a white noise signal. a_i and b_j are model parameters, with $i = 1 \ldots na$ and $j = 1 \ldots nb$. The model structure is entirely defined by the three integers na, nb, and nk.

The purpose of this section is to identify which image analysis parameters characterize the SVI evolution via *dynamic* ARX models. This is done by simulating the ARX models with organic loading (Q) and/or digital image analysis information parameters and analyzing prediction system performance based on the chosen criterion, R^2_{adj}. ARX models are identified by using the `arx` command in the System Identification Toolbox 5.0.1 in MATLAB (The Mathworks, Inc., Natick), which allows to specify a specific *focus* during model identification. Three different options are available, i.e., a focus on *prediction*, *simulation* or *stability*. *Prediction* means that the model is determined by minimizing the prediction errors. With focus on *simulation*, the model approximation is such that the model will produce as good simulations as possible, when applied to inputs with the same spectra as used for the estimation. A stable model is guaranteed. Finally, a *stability* focus implies that the algorithm is modified so that a stable model is guaranteed, but the weighting still corresponds to prediction. Previous studies (Banadda *et al.*, 2003), have shown that the performance of the optimal models with focus on *prediction* in combination with our own stability check is as good and sometimes even better than that of the models resulting from the *stability* focus. Therefore, identification results of the latter are omitted.

Space does not allow to show all the identification and validation results but both Tables 1 and 2 give a representative view on the identification and validation outcomes for ARX and state space models, respectively. Optimal combinations (organic loading and image analysis information)

were sought in the range of 1 to 5 for the number of poles (na) and zeros (nb) (with nb smaller than or equal to na) at fixed delays nk of 0, 1 and 2. The maximum value for na is deliberately kept low to avoid overfitting.

Identification and validation results.

One input case. F as a single input performs best in both identification and validation although other inputs such as Q can be reasonable in identification (e.g., for the first experiment) but validate badly. This result encourages the use of image analysis as an activated sludge monitoring tool.
Two input case. The input F in combination with another input is reasonable in identification and validation (except the validation with [F Q] in the first experiment). Excluding F as an input has a severe (negative) impact on the validation quality of the model. Overall, a combination of F and D_{eq} is a satisfying input combination.
Remarkably, the nk value is always equal to zero for F in the first experiment. For the second experiment, this nk value can deviate from zero but only in the multi-input case in combination with the input Q. These models are only a tenth of a percent better in identification but validate obviously rather bad on the first experiment. Therefore, in the search for optimal models for the data of the second experiment, the nk value corresponding to F is restricted to zero.
Three input case. No positive validation results are recorded except in the case of the [F D_{eq} Q] input combination for the second experiment model on the first experiment data. Relatively, good validation results are noted when F is one of the inputs. In general, [F D_{eq} Q] is a well performing input combination. Figure 3 shows the performance of the ARX models in identification (R^2_{adj} = 78.87%, second experiment) and validation (R^2_{adj} = 85.00%, first experiment) as compared to the measured SVI.

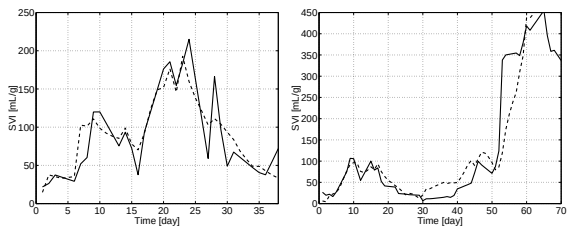

(a) (b)

Fig. 3. Measured SVI (—) and modeled SVI (- - -) with the optimal 1st-order ARX model and 3 model inputs [F D_{eq} Q] during (a) identification and (b) validation.

3.3 State space models

Procedure. Apart from ARX models, also state space models have been explored. In discrete time, a state space model has the following form

$$\begin{aligned} x(t+1) &= Ax(t) + Bu(t) + Ke(t) \\ y(t) &= Cx(t) + Du(t) + e(t) \end{aligned} \tag{8}$$

with $x(t)$ equal to the state vector at discrete time t, $y(t)$ equal to the output response, $u(t)$ the input, $e(t)$ a white noise signal, and A, B, C, D and K the state space matrices of appropriate dimensions.

In this section, state space models are identified by means of the `n4sid` command in the System Identification Toolbox 5.0.1 in MATLAB (The Mathworks, Inc., Natick), which allows, similar to the ARX command, to choose a specific *focus* during model identification. `n4sid` is a subspace-based method that does not use iterative search. As for ARX modeling, optimal combinations of the organic loading and image analysis information (state space model inputs) for both the first and the second experiment were sought in the order range of 1 to 4 and their performance evaluated based on the R^2_{adj} criterion (Equations (6)).

Identification and validation results.

One input case. As for ARX modeling, again F as a single input performs best in identification and validation while other inputs such as Q show relatively lower identification values and validate badly.
Two input case. For the first experiment, no positive validation results are obtained. As for the second experiment, F must be in it; [F D_{eq}] or [F Q] are appropriate input combinations.
Three input case. For the first experiment, no positive validation results are noted. For the second experiment, F must be in it and this in combination with Q or D_{eq}, with [F D_{eq} Q] giving the highest validation results on the first experiment. Figure 4 elucidates the performance of the state space models in identification (R^2_{adj} = 69.56%, second experiment) and validation (R^2_{adj} = 80.29%, first experiment) as compared to the measured SVI.

3.4 Discussion

Several interesting *general* remarks remain to be stated. They are listed below.

- The validation performance of the single input model with F is as good as, or at times better than that of some given multi-input models but the latter are most often better in identification. However, from a *prediction*

Table 1. Optimal ARX model output with 1, 2 or 3 model input(s) for the first experiment and the second experiment.

Focus	Model				R^2_{adj} (%)					R^2_{adj} (%)	
on	inputs	na	nb	nk	ARX^1	ARX^{1-2}	na	nb	nk	ARX^2	ARX^{2-1}
Prediction	F	5	1	0	79.89	54.49	1	1	0	67.85	84.29
	Q	1	1	2	62.04	-51.28e+01	5	1	0	12.55	-56.52e-01
	F, Q	5	[1 5]	[0 2]	82.66	-70.93	1	[1 1]	[0 2]	72.27	86.00
	F, AR	5	[1 1]	[0 2]	79.04	52.02	1	[1 1]	[0 0]	71.55	75.15
	F, D_{eq}	5	[1 1]	[0 1]	79.57	53.09	1	[1 1]	[0 0]	71.81	76.20
	Q, D_{eq}	5	[2 5]	[1 2]	78.34	-86.93e+01	5	[2 1]	[0 2]	32.33	-18.43
	AR, D_{eq}	5	[1 5]	[2 1]	63.92	-18.31e+02	3	[1 1]	[0 0]	48.87	79.50e-01
	F, D_{eq}, Q	5	[3 5 2]	[0 2 1]	91.23	-61.06e+01	1	[1 1 1]	[0 0 2]	78.87	85.00
	F, FF, R	5	[3 5 2]	[0 2 0]	88.80	-11.78e+02	3	[3 1 1]	[0 0 0]	78.84	-79.71
	F, FF, RG	4	[3 2 1]	[0 1 2]	87.25	-77.57e+01	2	[2 1 1]	[0 0 0]	74.06	-10.94
	F, FF, AR	5	[3 5 2]	[0 2 1]	88.42	-15.63e+02	4	[1 3 2]	[0 1 2]	77.08	-80.86e-01
Simulation	F	4	4	0	83.83	57.59	2	1	0	67.48	82.36
	Q	1	1	2	64.58	-42.83e+01	2	1	0	26.30	38.25e-01
	F, Q	4	[3 2]	[0 0]	92.57	-12.30e+01	5	[1 4]	[0 1]	75.63	78.76
	F, AR	3	[3 2]	[0 2]	85.03	58.74	1	[1 1]	[0 0]	73.52	33.89
	F, D_{eq}	3	[3 1]	[0 2]	83.60	46.04	1	[1 1]	[0 0]	71.99	66.58
	Q, D_{eq}	3	[3 3]	[2 2]	90.58	-10.80e+02	5	[1 2]	[0 2]	74.79	-14.58
	AR, D_{eq}	4	[1 2]	[2 0]	86.77	-61.42e+02	1	[1 1]	[0 1]	55.17	16.87
	F, D_{eq}, Q	3	[3 3 2]	[0 2 0]	94.74	-45.62e+01	1	[1 1 1]	[0 0 2]	79.47	81.63
	F, FF, R	4	[4 4 4]	[0 2 2]	95.85	-89.23e+01	3	[3 1 1]	[0 0 0]	79.50	-85.03
	F, FF, RG	5	[3 5 5]	[0 2 2]	96.16	-65.39e+01	3	[1 2 2]	[0 0 0]	76.65	-82.60
	F, FF, AR	5	[4 5 5]	[0 2 2]	96.14	-13.59e+02	4	[1 2 3]	[0 2 1]	77.21	-52.06
	FF, R, AR	2	[2 1 2]	[2 1 2]	94.21	-42.21e+02	3	[1 3 2]	[0 0 1]	81.68	-16.50+01

ARX^{1-2}: R^2_{adj} values of ARX models identified from the first experiment (ARX^1) and validated on the second experiment.
ARX^{2-1}: R^2_{adj} values of ARX models identified from the second experiment (ARX^2) and validated on the first experiment.

Table 2. Optimal state space model output with 1, 2 or 3 model input(s) for the first experiment and the second experiment.

Focus	Model	Optimal	R^2_{adj} (%)		Optimal	R^2_{adj} (%)	
on	inputs	order	ss^1	ss^{1-2}	order	ss^2	ss^{2-1}
Prediction	F	3	73.05	40.81	1	59.75	79.68
	Q	2	59.19	-704.47	1	0.20	1.34
	F, Q	2	65.41	-48.43e+01	1	65.60	76.47
	F, AR	2	55.25	-13.02	1	57.22	76.87
	F, D_{eq}	4	71.08	-20.63e–01	1	60.04	79.28
	Q, D_{eq}	1	74.92	-32.67e+01	3	33.25	-30.09
	AR, D_{eq}	2	73.26	-13.89e+02	3	54.82	15.07e-02
	F, D_{eq}, Q	2	75.41	-33.52e+01	1	69.56	80.29
	F, FF, R	1	62.67	-64.26e+01	1	64.33	98.16e-01
	F, FF, RG	1	63.89	-45.15e+01	1	60.36	21.91
	F, FF, AR	1	66.49	-59.13e+01	1	64.55	-25.35
	FF, R, AR	1	59.50	-54.32e+01	1	64.07	-11.44e+01
Simulation	F	2	83.14	-12.64	1	61.47	80.03
	Q	2	67.09	-2.41e+03	2	25.31	-13.08
	F, Q	4	88.12	-24.11e+02	1	66.65	79.58
	F, AR	3	83.35	-60.24e+01	1	61.91	73.17
	F, D_{eq}	2	83.01	-18.32	1	63.46	74.87
	Q, D_{eq}	3	92.18	-15.62e+02	3	48.35	-28.56
	AR, D_{eq}	2	83.37	-17.76e+02	3	57.26	26.54e-01
	F, D_{eq}, Q	2	89.03	-34.46e+01	1	70.54	79.95
	F, FF, R	4	87.22	-32.47e+01	1	64.71	30.22e-01
	F, FF, RG	4	88.78	-39.37e+01	1	62.61	51.46
	F, FF, AR	3	88.11	-25.86e+01	1	65.85	-49.56e-01
	FF, R, AR	2	94.30	-13.95e+02	2	66.71	-17.11e+01

ss^{1-2}: R^2_{adj} values of state space models identified from the first experiment (ss^1) and validated on the second experiment.
ss^{2-1}: R^2_{adj} values of state space models identified from the second experiment (ss^2) and validated on the first experiment.

point of view, the filament length input is less suitable since the n_k value is equal to zero, indicating a change in the parameter *at the same time* as the change in the SVI.

- Validation of the models identified on the data of the first experiment is bad or non existing. This could be due to the fact that too much effort has been dedicated in identifying the SVI jump, i.e., values in the range of 250mLg^{-1} to 450mLg^{-1} during the first experiment, a jump that is not present in the second experiment.
- If the second experiment models validate well on data of the first experiment, the R^2_{adj} criterion value is for yet unexplainable reasons higher in validation than in identification. This is also true for the R^2 criterion that does not compensate for the number of data points and the number of degrees of freedom (results not shown).
- Most often, combinations of F, FF, Q and D_{eq} with the floc elongation related parameters R, RG or AR give rise to more or less similar identification values, implying that

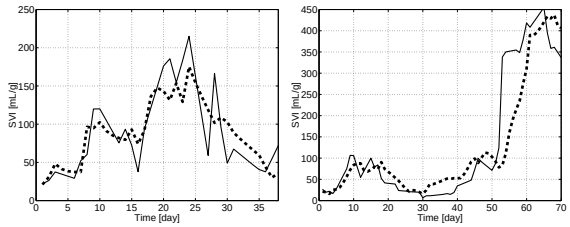

(a) (b)

Fig. 4. Measured SVI (—) and modeled SVI (- - -) with the optimal 1st-order state space model and 3 model inputs [F D_{eq} Q] during (a) identification and (b) validation.

probably only one of the roundness related floc characteristics will be sufficient.

- A final remark is related to the MATLAB implementation. Although not needed, we did test the model stability when implementing the *simulation* focus. We then noticed that the System Identification Toolbox is rather generous in assigning the stable label to a model. Models, whose poles lie within a circle of a radius of 1.01, are regarded as stable by MATLAB.

4. CONCLUSIONS

In the quest for an early forecast tool for filamentous bulking in activated sludge wastewater treatment systems, organic loading and/or digital image analysis information have been exploited into dynamic black box models to predict the Sludge Volume Index evolution based on a quality performance criterion, i.e., R^2_{adj}. If the floc and filament characteristics change *before* the SVI reaches its critical limit, a *dynamic* model, taking into account previous input and output values, could aid in predicting filamentous bulking before it really happens, which is not feasible with static, instantaneous models. Therefore, ARX and state space models were identified from two individual data sets and afterwards cross-validated on the data of the other experiment.

ARX models are better (higher criterion values) in identification than state space models and as good in validation. Previous studies have earmarked image analysis information as a promising activated sludge monitoring tool (Jenné *et al.*, 2003). In this paper this conclusion is confirmed. An interesting observation is, e.g., that the total filament length per image (F) could either be used as a single input or in combination with other (floc related) inputs, especially if good validation quality is to be attained. The validation exercise with a single input shows F as a strong candidate to model the SVI behavior as compared to Q. [F D_{eq}] and [F D_{eq} Q] come out as well performing multi-input combinations though the validation results with a single input F are equally good. The drawback of the filament length as an input is the lack of *predictive* power since the characteristic changes occur at the same time as the change in the SVI values. As additional experimental data and other image analysis based model inputs become available, re-identification and further validation of ARX models will be performed.

ACKNOWLEDGEMENTS

Work supported by Projects OT/99/24, OT/03/30 and IDO/00/008 of the KULeuven Research Council, and the Belgian Program on Interuniversity Poles of Attraction, initiated by the Belgian Federal Science Policy Office. Ilse Smets is a postdoctoral fellow with the fund for Scientific Research Flanders. The scientific responsibility is assumed by its authors.

REFERENCES

Banadda, E.N., R. Jenné, I.Y. Smets and J. F. Van Impe (2003). Predicting the onset of filamentous bulking in biological wastewater treatment systems by exploiting image analysis information. European Control Conference ECC2003 CD ROM 6p, University of Cambridge, UK.

da Motta, M., M.N. Pons and N. Roche (2002). Study of filamentous bacteria by image analysis and relation with settleability. *Water Science and Technology* **46**, 363–369.

Eriksson, L. and A.M. Hardin (1984). Settling properties of activated sludge related to floc structure. *Water Science and Technology* **16**(10-11), 55–68.

Ganczarczyk, J.J. (1994). Microbial aggregates in wastewater treatment. *Water Science and Technology* **30**(8), 87–95.

Jenkins, D., M. G. Richard and G. T. Daigger (1993). *Manual on the causes and control of activated sludge bulking and foaming.* 2nd edition. Lewis. London (UK).

Jenné, R., C. Cenens, A.H. Geeraerd and Van Impe J.F. (2002). Towards on-line quantification of flocs and filaments by image analysis. *Biotechnology Letters* **24**(11), 931–935.

Jenné, R., E.N. Banadda, N. Philips and J. F. Van Impe (2003). Image analysis as a monitoring tool for activated sludge properties in lab-scale installations. *Environmental Science and Health Part A* **38**(10), 2009–2018.

Novotny, V., H. Jones, X. Feng and A.G. Capodaglio (1990). Time series analysis models of activated sludge plants. *Water Science and Technology* **23**, 1107–16.